J Math Chem (2010) 48:347–362
DOI 10.1007/s10910-010-9675-5

ORIGINAL PAPER

New features of the steady-state rate related with the initial concentration of substrate in the diphenolase and monophenolase activities of tyrosinase

Jose Luis Muñoz-Muñoz · Francisco Garcia-Molina · Ramón Varon · Jose Tudela · Francisco Garcia-Cánovas · Jose N. Rodríguez-López

Received: 22 February 2010 / Accepted: 23 March 2010 / Published online: 11 April 2010
© Springer Science+Business Media, LLC 2010

Abstract Tyrosinase has two types of enzymatic activities: the hydroxylation of monophenols to *o*-diphenols (monophenolase activity) and oxidation of *o*-diphenols to *o*-quinones (diphenolase activity). The action on *o*-diphenols involves two substrates: oxygen and *o*-diphenol, while the mechanism proposed is a Uni Uni Bi Bi ping-pong. In this contribution, we demonstrate experimentally that there is a kinetically preferred pathway, which translates into the appearance of curves of initial velocity *vs*. initial diphenol concentration shows inhibition by an excess of substrate, while sigmoid curves are obtained when the initial velocity *vs*. initial oxygen concentration are graphed. However, the action mechanism of the enzyme on monophenols, which is more complex because it involves three substrates (monophenol, oxygen and *o*-diphenol), does behave differently from the hyperbolic behaviour as regards the initial velocity *vs*. initial monophenol concentration, results that can be explained if the limiting step in the action of tyrosinase is the hydroxylation of monophenol to *o*-diphenol.

Keywords Tyrosinase · Kinetically preferred pathway · Slow pathway · Diphenolase activity · Monophenolase activity

J. L. Muñoz-Muñoz · F. Garcia-Molina · J. Tudela · F. Garcia-Cánovas (✉) · J. N. Rodríguez-López
GENZ: Grupo de Investigación Enzimología, Departamento de Bioquímica y Biología Molecular-A, Facultad de Biología, Universidad de Murcia, 30100 Espinardo, Murcia, Spain
e-mail: canovasf@um.es

R. Varon
Departamento de Química-Física, Escuela de Ingenieros Industriales de Albacete, Universidad de Castilla la Mancha, Avda. España s/n. Campus Universitario, 02071 Albacete, Spain

1 Introduction

It has long been known that cooperativity is not an exclusive characteristic of oligomeric enzymes, and two models have been proposed to explain the phenomenon: binding equilibrium models and kinetic models [1–3]. The simplest models are kinetic since, in them, a monomer with only one active site is capable of deviating from hyperbolic behaviour and showing sigmoidal behaviour when the concentration of substrate is varied [3]. Among enzymes which have been seen to deviate from the hyperbolic are: phosphofructokinase [4], isocitrate dehydrogenase of yeast [5] and heart malic dehydrogenase [6].

Tyrosinase (TYR: monophenol, *o*-diphenol; oxygen-oxidoreductase; EC 1.14.18.1) has two copper atoms in its active site and is ubiquitously present in biological systems [7]. It catalyzes the oxidation of *o*-diphenols (*o*-diphenolase or catecholase activity) to the corresponding *o*-quinones, through the consumption of molecular oxygen. It may also catalyze the regioselective ortho-hydroxylation of monophenols to catechols (monophenolase or cresolase activity) and their subsequent oxidation to *o*-quinones. The catalytic centre of tyrosinase possesses a binuclear copper similar to that of hemocyanin and catechol oxidase [7]. The catalytic cycle of tyrosinase has three enzymatic forms: E_m (*met*-tyrosinase), with the copper as $Cu^{2+}Cu^{2+}$, E_d (*deoxy*-tyrosinase), with the copper as $Cu^{+}Cu^{+}$ and E_{ox} (*oxy*-tyrosinase) with copper in the form $Cu^{2+}Cu^{2+}O_2^{2-}$ [8]. In the structure of tyrosinase from *Streptomyces castaneoglobisporus* [9], each copper ion is coordinated by three histidines (2 histidines in equatorial position and one in axial position) [9–11].

The action mechanism of tyrosinase on *o*-diphenols and monophenols has been widely studied [7,12]. The mechanism is complex since the enzyme exists in three forms in the catalytic cycle (*met*-tyrosinase, *deoxy*-tyrosinase and *oxy*-tyrosinase), while the reaction product, *o*-quinone, is unstable. The development of suitable methods to measure each of these activities [13] and the characterisation of the kinetic mechanism of the enzyme acting on diphenols and monophenols [7,14] has increased our understanding of the melanin biosynthesis pathway [15,16].

This work uses kinetic studies of the steady-state of both activities (monophenolase and diphenolase), to (1) detect the limiting step of the process, (2) explain the inhibition by an excess of *o*-diphenol in diphenolase activity, (3) explain the generation of a sigmoid curve when the oxygen concentration in diphenolase activity is varied, (4) interpret the absence of inhibition by excess monophenol in the monophenolase activity when the concentration of monophenol is varied and (5) explain the absence of a sigmoid curve when the oxygen concentration in monophenolase activity is varied.

1.1 Abbreviation

For clarity and for the sake of brevity, the following additional notations will be used in the text.

1.1.1 Species and concentrations

D	Diphenol (L- and D-dopa)
M	Monophenol (L- and D-tyrosine)
E	Enzyme (tyrosinase)
$[E]_0$	Initial concentration of enzyme

1.1.2 Kinetic parameters

V_0^D	Initial rate of tyrosinase acting on D
V_0^M	Initial rate of tyrosinase acting on M
$V_{\max}^D$	Maximal rate of tyrosinase for D
$V_{\max}^M$	Maximal rate of tyrosinase for M
k_{cat}^D	Catalytic constant of tyrosinase acting on D
k_{cat}^M	Catalytic constant of tyrosinase acting on M
$K_m^{D(P)}$	Apparent Michaelis constant of tyrosinase for D in the kinetically preferred pathway
$K_m^{M(P)}$	Apparent Michaelis constant of tyrosinase for M in the kinetically preferred pathway
$K_{m,D}^{O_2(P)}$	Apparent Michaelis constant for O_2 in the diphenolase activity in the kinetically preferred pathway
$K_{m,D}^{O_2(S)}$	Apparent Michaelis constant for O_2 in the diphenolase activity in the slow pathway
$K_{m,M}^{O_2(P)}$	Apparent Michaelis constant for O_2 in the monophenolase activity on the kinetically preferred pathway
$K_{m,M}^{O_2(S)}$	Apparent Michaelis constant for O_2 in the monophenolase activity on the slow pathway

2 Experimental

2.1 Reagents

Commercial mushroom tyrosinase (TYR) and the substrates used in this work (L- and D-dopa and L- and D-tyrosine) were purchased by Sigma (Madrid). Other chemicals were of analytical grade and supplied by Merck (Darmstadt, Germany). Stock solutions of the diphenolic and monophenolic substrates were prepared in 0.15 mM phosphoric acid to prevent autooxidation. Milli-Q system (Millipore corp.) ultrapure water was used throughout.

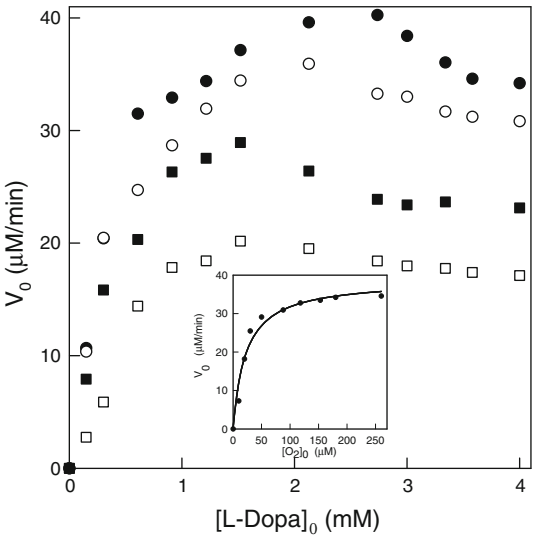

Fig. 1 Representation of the initial velocity values obtained for action of TYR on different initial concentration of *o*-diphenol, at different concentrations of oxygen. The experimental conditions were: 30 mM sodium phosphate buffer (pH 7.0), 25 °C, $[E]_0 = 6$ nM and the initial oxygen concentrations were (μM): (*filled circle*) 260, (*open circle*) 100, (*filled square*) 30 and (*open square*) 20. The L-dopa concentrations (mM) were varied as indicated in the figure. *Inset* Representation of the initial velocity *vs.* initial concentration of O_2, at L-dopa concentration of 4 mM and $[E]_0 = 6$ nM

2.2 Enzyme source

Mushroom tyrosinase was purified by Duckworth and Coleman's procedure but with two additional chromatographic steps [17]. The enzyme solution was passed through a column (2.0 × 30 cm) of Sephadex G-100 (Pharmacia) equilibrated on 0.01 M sodium phosphate buffer (pH 7). Samples showing tyrosinase activity were further purified by FPLC anion-exchange chromatography on a Mono-Q HR 5/5 column (2.0 × 30 cm) (Pharmacia) equilibrated with 0.01 M sodium phosphate (pH 7) and eluted with sodium chloride (0–0.5 M gradient). Purified enzyme was desalted with Sephadex G-25 (Pharmacia) into ultrapure water and stored in liquid nitrogen. Protein concentration was determined by Bradford's method [18], using bovine serum albumin as standard.

2.3 Spectrophotometric assays

These assays were carried out with a Perkin-Elmer Lambda-35 spectrophotometer, on line interfaced to a PC-computer, where the kinetic data were recorded, stored and later analyzed. The product of the enzyme reaction, the *o*-quinone, is not suitable for experimental detection at long assay times due to the instability of the *o*-quinones [19,20], and so the experimental assays were made at short times. The reaction was followed by measuring: (a) the disappearance of NADH at 340 nm with $\varepsilon = 6,230\ \mathrm{M^{-1}\ cm^{-1}}$, (L- and D-dopa) [13] and (b) the appearance dopachrome accumulation at 475 nm with $\varepsilon = 3600\ \mathrm{M^{-1}\ cm^{-1}}$ (L- and D-tyrosine) [21]. The cuvette (final volume 1 ml) contained $[\mathrm{NADH}]_0 = 0.2$ mM for the measurement with *o*-diphenols and 30 mM sodium phosphate buffer (pH 7.0) (monophenols and *o*-diphenols). The initial substrate (monophenol and *o*-diphenol) and oxygen concentrations were varied as indicated in the legends of Figs. 1 and 3. The reaction was started with the addition of enzyme.

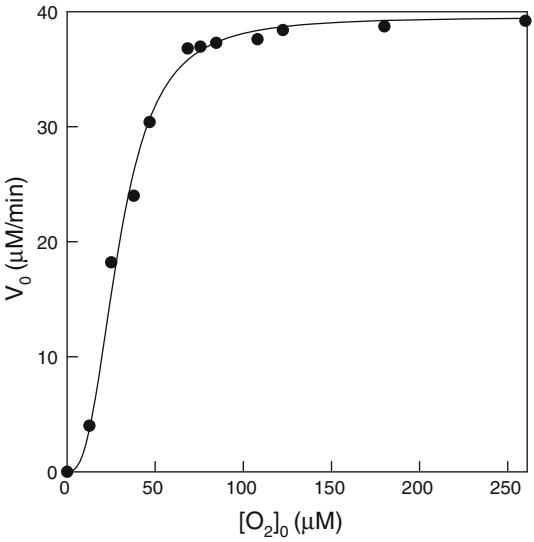

Fig. 2 Representation of the initial velocity values obtained for action of TYR on a fixed concentration of L-dopa (2.8 mM), varying the initial concentration of oxygen. The experimental conditions were: 30 mM sodium phosphate buffer (pH 7.0), 25 °C and $[E]_0 = 6$ nM. The O_2 concentrations (μM) were varied as indicated in the figure

2.4 Oxymetric assays

Measurements of dissolved oxygen concentration were made with a Hansatech (Kings Lynn, Cambs, UK) oxygraph unit controlled by a PC. The oxygraph used a Clark-type silver/platinum electrode with a 12.5 μm Teflon membrane. The sample was continuously stirred during the experiments and its temperature was maintained at 25 °C. The zero oxygen level for calibration and experiments was obtained by bubbling oxygen-free nitrogen through the sample for at least 10 min [22]. The cuvette (final volume 2 ml) contained 30 mM sodium phosphate buffer (pH 7.0) and monophenol and *o*-diphenol at a concentration at which tyrosinase is saturated by them. The initial oxygen concentration was varied as is indicated in the legends of Figs. 2 and 4.

2.5 Kinetic data analysis

V_0-values were calculated from triplicate measurements at each reducing substrate concentration. The fitting was carried out using the Sigma Plot 9.0 program for Windows [23], obtaining $V_{\max}$ and K_m^S by non-linear regression to the Michaelis-Menten equation.

3 Results and discussion

Mushroom tyrosinase (EC 1.14.18.1) is an enzyme that contains copper in its active centre and which catalyzes the hydroxylation of monophenols to *o*-diphenols (monophenolase activity) and the oxidation of *o*-diphenols to their corresponding *o*-quinones (diphenolase activity) in a reaction in which molecular oxygen intervenes [7]. We shall first look at diphenolase activity.

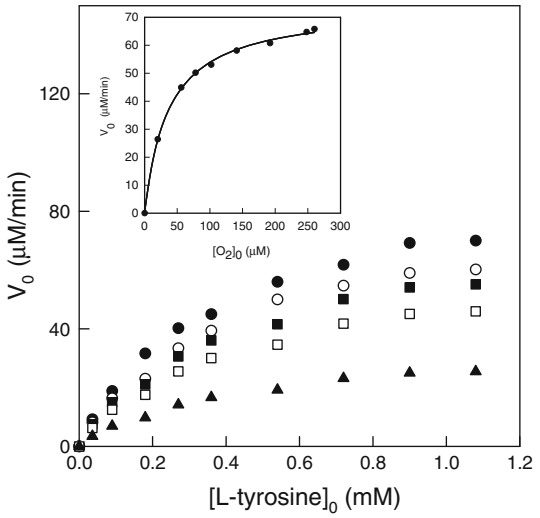

Fig. 3 Representation of the initial velocity values obtained for action of TYR on different initial concentrations of L-tyrosine at different initial concentrations of oxygen. The experimental conditions were: 30 mM sodium phosphate buffer (pH 7.0), 25 °C, $[E]_0 = 145$ nM and the initial oxygen concentrations (μM) were: (*filled circle*) 260, (*open circle*) 200, (*filled square*) 100, (*open square*) 50 and (*open triangle*) 20. The L-tyrosine concentrations (mM) were varied as indicated in the figure. *Inset* Representation of the initial velocity at an initial L-tyrosine concentration of 1.1 mM and different initial concentrations of oxygen. The experimental conditions were the same as in Fig. 3

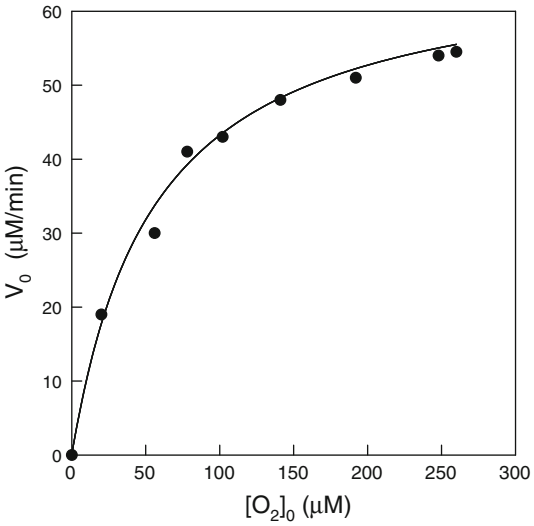

Fig. 4 Representation of the initial velocity values obtained for TYR acting on L-tyrosine (0.54 mM), varying the initial oxygen concentration. The experimental conditions were: 30 mM sodium phosphate buffer (pH 7.0), 25 °C and $[E]_0 = 145$ nM. The O_2 concentrations (μM) were varied as indicated in the figure

3.1 Diphenolase activity

The mechanism proposed to explain diphenolase activity is described in Scheme 1. Enzyme turnover begins with *met*-tyrosinase, which reacts with *o*-diphenol (D) to form the complex *met*-tyrosinase/diphenol. The *o*-diphenol is oxidised to *o*-quinone

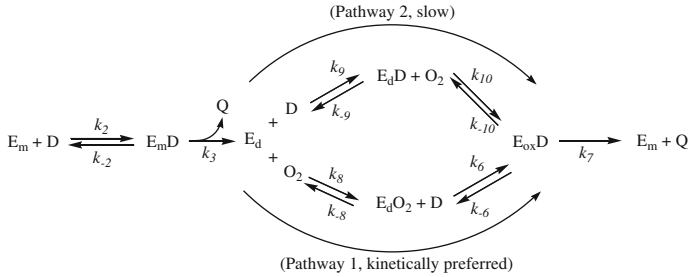

Scheme 1 Kinetic mechanism proposed to explain the action of tyrosinase on *o*-diphenols. E_m, *met*-tyrosinase; E_d, *deoxy*-tyrosinase; E_{ox}, *oxy*-tyrosinase; D, *o*-diphenol; Q, *o*-quinone; $E_m D$, *met*-tyrosinase/*o*-diphenol complex; $E_d D$, *deoxy*-tyrosinase/*o*-diphenol complex; $E_d O_2$; *deoxy*-tyrosinase/oxygen complex; $E_{ox} D$, *oxy*-tyrosinase/*o*-diphenol complex

and the form *deoxy*-tyrosinase is generated. This form, with Cu^+Cu^+, can react with O_2 to give *oxy*-tyrosinase, which, when it reacts with the *o*-diphenol, forms *oxy*-tyrosinase/diphenol, which, in turn, is transformed into *met*-tyrosinase and *o*-quinone. The pathway described (pathway 1) in the mechanism of Scheme 1 is the normal pathway followed by the enzyme. However, at high concentrations of *o*-diphenol, the *deoxy*-tyrosinase form can bind to it before the oxygen to form a *deoxy*-tyrosinase/*o*-diphenol complex, which subsequently binds to the O_2, giving rise to a new form, *oxy*-tyrosinase/*o*-diphenol, which is transformed into *met*-tyrosinase and *o*-quinone (pathway 2, slow).

The experimental data for the initial velocity *vs.* initial *o*-diphenol (substrate) concentration, Fig. 1, shows that the pathways described above differ kinetically, so that pathway 1 should be kinetically preferred and pathway 2 slow. Note that inhibition by excess of substrate occurs earlier at low O_2 concentrations, that is, at the lowest concentrations of *o*-diphenol. Figure 1 Inset shows the initial velocity obtained at a fixed initial concentration of *o*-diphenol (high) and varying the initial concentration of oxygen.

A kinetic study of the kinetically preferred pathway gives the values of $K_m^{D(P)}$, the apparent Michaelis constant for the *o*-diphenol in the kinetically preferred pathway, and k_{cat}^D, the catalytic constant. The analytical expressions according to [14] are:

$$K_m^{D(P)} = k_{\text{cat}}^D / k_6 \tag{1}$$

and

$$k_{\text{cat}}^D = \frac{k_3 k_7}{k_3 + k_7} \tag{2}$$

The Michaelis constant for oxygen is:

$$K_{m,D}^{O_2(P)} = k_{\text{cat}}^D / k_8 \tag{3}$$

Figure 1 Inset shows the initial velocity obtained at a high concentration of *o*-diphenol (and different concentrations of oxygen). From these data, the apparent Michaelis constant for oxygen in the slow pathway can be obtained:

$$K_{m,D}^{O_2(S)} = k_{\text{cat}}^{D}/k_{10} \tag{4}$$

The data showed in Table 1 and Fig. 1 indicate that the mechanism is dependent of the oxygen concentration because the apparent Michaelis constant for oxygen increased from the Eq. (3)-value to the Eq. (4)-value (see Table 1).

Figure 2 shows the values of the initial velocity obtained at a fixed concentration of *o*-diphenol and increasing initial concentrations of oxygen. The sigmoid shape is similar to that obtained with the enzyme phosphofructokinase [24], behaviour which can be explained, according to Scheme 1, if two pathways exist to reach the intermediate *oxy*-tyrosinase/*o*-diphenol, $E_{ox}D$, starting from *deoxy*-tyrosinase, E_d. As indicated by Ferdinand [3], an indicative test for kinetically preferred pathway, in a bisubstrate reaction, includes inhibition by excess of substrate (*o*-diphenol in this case) and sigmoicidity with respect to the other substrate (oxygen in this case).

Therefore, at fixed concentration of oxygen, the velocity increases as the initial concentration of *o*-diphenol increases until it binds to the form *deoxy*-tyrosinase, entering the slow pathway and inhibition through excess substrate occurs (Fig. 1). In the case described in Fig. 2, at low initial concentrations of oxygen and high concentrations of *o*-diphenol, the enzyme follows pathway 2 and, as oxygen is added, it takes the kinetically preferred pathway and a sigmoid curve is obtained. From these experimental results, it can be deduced that the mechanism described in Scheme 1 does not reach rapid equilibrium but passes through a steady-state, since the velocity expression with respect to initial *o*-diphenol concentration and in the case of rapid equilibrium is a hyperbola, Eq. 5 (expressions $\alpha_1 - \alpha_4$ are given in Appendix), is:

$$\frac{V_0}{[E]_0} = \frac{\alpha_1[D]_0[O_2]_0}{\alpha_2 + \alpha_3[O_2]_0 + \alpha_4[D]_0 + [D]_0[O_2]_0} \tag{5}$$

which does not agree with the experimental results. This leads us to conclude that the mechanism reaches a steady-state so that the velocity equation of the mechanism would correspond to Eq. (6). Expressions $\beta_1 - \beta_{11}$ are given in the Appendix.

$$\frac{V_0}{[E]_0} = \frac{\beta_1[D]_0[O_2]_0 + \beta_2[D]_0[O_2]_0^2 + \beta_3[D]_0^2[O_2]_0}{\beta_4 + \beta_5[O_2]_0 + \beta_6[D]_0 + \beta_7[O_2]_0^2 + \beta_8[D]_0[O_2]_0 + \beta_9[D]_0^2 + \beta_{10}[D]_0[O_2]_0^2 + \beta_{11}[D]_0^2[O_2]_0} \tag{6}$$

3.2 Monophenolase activity

The mechanism that describes the monophenolase activity of tyrosinase is described in Scheme 2. In this case, too, the binding of monophenol to de*oxy*-tyrosinase was considered, and the pathway was seen to be slow. However, since the steady-state concentration of *o*-diphenol is low, so that $[D]_0/[M]_0 = R = 0.046$ [25], it is assumed that, in this case, D does not bind to the *deoxy*-tyrosinase. The velocity equation for the

Table 1 Kinetic constants and parameters obtained for action of TYR on isomers of dopa and tyrosine

Substrate	$K_m^{S(P)}$ (mM)	$K_m^{O_2(P)}$ (μM)	$K_m^{O_2(S)}$ (μM)	k_{cat} (s^{-1})	$k_6 \times 10^{-5}$ ($M^{-1}s^{-1}$)	$k_4 \times 10^{-3}$ ($M^{-1}s^{-1}$)	$k_8 \times 10^{-7}$ ($M^{-1}s^{-1}$)	$k_{10} \times 10^{-6}$ ($M^{-1}s^{-1}$)
L-dopa	0.50 ± 0.06	4.78 ± 0.72	28 ± 4	110.0 ± 10.2	2.20 ± 0.32	–	2.3 ± 0.4	3.93 ± 0.88
D-dopa	2.15 ± 0.28	4.57 ± 0.68	31 ± 2	105.3 ± 10.4	0.48 ± 0.08	–	2.3 ± 0.4	3.39 ± 0.66
L-tyrosine	0.27 ± 0.03	0.53 ± 0.07	37 ± 2	8.1 ± 1.4	–	30.0 ± 4.1	2.3 ± 0.4	–
D-tyrosine	1.21 ± 0.16	0.52 ± 0.08	40 ± 4	7.9 ± 1.9	–	6.5 ± 1.2	2.3 ± 0.4	–

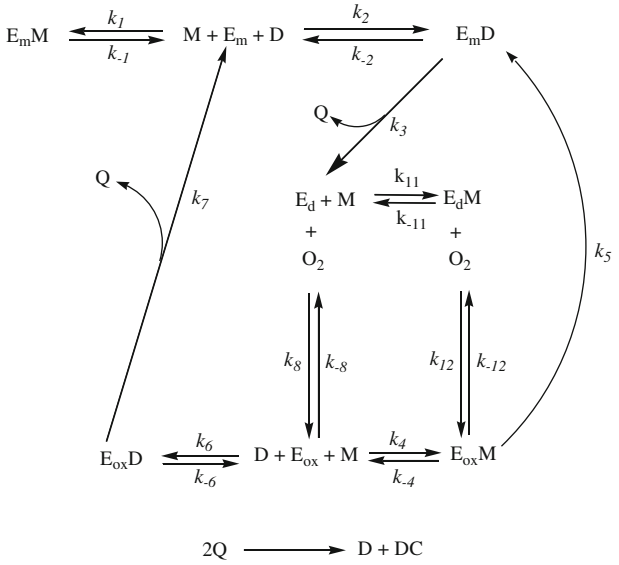

Scheme 2 Kinetic mechanism proposed to explain the action of tyrosinase on monophenols. E_m, *met*-tyrosinase; E_d, *deoxy*-tyrosinase; E_{ox}, *oxy*-tyrosinase; D, *o*-diphenol; Q, *o*-quinone; M, monophenol; $E_m M$, *met*-tyrosinase/monophenol complex; $E_m D$, *met*-tyrosinase/*o*-diphenol complex; $E_d M$, *deoxy*-tyrosinase/monophenol complex; $E_{ox} M$, *oxy*-tyrosinase/monophenol complex; $E_{ox} D$, *oxy*-tyrosinase/*o*-diphenol complex

mechanism of Scheme 2, accepting that the steady-state is reached, is Eq. (7), where a 3:3 ratio exists for the monophenol between the numerator and the denominator. The analytical expressions for $\gamma_1 - \gamma_{21}$ are given in the Appendix.

$$\frac{V_0}{[E]_0} = \frac{\begin{array}{c}\gamma_1[O_2]_0[M]_0^2 + \gamma_2[O_2]_0[D]_0[M]_0 + \gamma_3[O_2]_0[M]_0^3 \\ + \gamma_4[O_2]_0^2[M]_0^2 + \gamma_5[D]_0[O_2]_0[M]_0^2 + \gamma_6[D]_0[O_2]_0^2[M]\end{array}}{\begin{array}{l}\gamma_7[M]_0 + \gamma_8[M]_0^2 + \gamma_9[O_2]_0[M]_0 + \gamma_{10}[D]_0[M]_0 \\ + \gamma_{11}[D]_0[O_2]_0 + \gamma_{12}[M]_0^3 + \gamma_{13}[O_2]_0[M]_0^2 + \gamma_{14}[O_2]_0^2[M]_0 \\ + \gamma_{15}[D]_0[M]_0^2 + \gamma_{16}[D]_0[O_2]_0[M]_0 + \gamma_{17}[D]_0[O_2]_0^2 + \gamma_{18}[O_2]_0[M]_0^3 \\ + \gamma_{19}[O_2]_0^2[M]_0^2 + \gamma_{20}[D]_0[O_2]_0[M]_0^2 + \gamma_{21}[D]_0[O_2]_0^2[M]_0\end{array}} \tag{7}$$

Furthermore, the experimental data for the initial velocity *vs*. substrate concentration (monophenol), Fig. 3, point to a hyperbolic behaviour. From these data, it can be deduced that the mechanism does not follow the steady-state model, but must follow the rapid equilibrium model, meaning that the equation is simpler. If we consider the step governed by k_5 (hydroxylation reaction) as the slow step of the turnover, the velocity equation takes a hyperbolic form, Eq. (8). The expressions for $\varphi_1 - \varphi_9$ are given in the Appendix.

$$\frac{V_0}{[E]_0} = \frac{\varphi_1[D]_0[O_2]_0[M]_0 + \varphi_2[D]_0^2[O_2]_0}{\varphi_3[D]_0 + \varphi_4[O_2]_0[M]_0 + \varphi_5[D]_0[M]_0 + \varphi_6[D]_0[O_2]_0 + \varphi_7[O_2]_0[M]_0^2 + \varphi_8[D]_0[O_2]_0[M]_0 + \varphi_9[D]_0^2[O_2]_0} \tag{8}$$

Since $[D]_0/[M]_0 = R$ [25], $[D]_0$ in Eq. (8) can be substituted by $R[M]_0$ so that the equation simplifies to Eq. (9):

$$\frac{V_0}{[E]_0} = \frac{\left[\varphi_1 R[O_2]_0 + \varphi_2 R^2[O_2]_0\right][M]_0}{\varphi_3 R + \varphi_4[O_2]_0 + \varphi_6[O_2]_0 + \left[\varphi_5 R + \varphi_7[O_2]_0 + \varphi_8 R[O_2]_0 + \varphi_9 R^2[O_2]_0\right][M]_0} \tag{9}$$

The results of the kinetic study with monophenols are shown in Table 1. When the initial concentration of oxygen is saturating, so that only the rapid pathway is followed, the apparent Michaelis constant for the monophenol can be obtained (see Table 1):

$$K_m^{M(P)} = k_{\text{cat}}^M / k_4 \tag{10}$$

and

$$k_{\text{cat}}^M = k_5 \tag{11}$$

The apparent Michaelis constant for oxygen is:

$$K_{m,M}^{O_2(P)} = \frac{3}{2} k_{\text{cat}}^M / k_8 \tag{12}$$

The data showed in Table 1 and Fig. 3 shows that the mechanism is dependent of the oxygen concentration because the apparent Michaelis constant for oxygen increased from the Eq. (12)-value to a more complex expression, which is shown in Eq. (A47) (see Appendix).

Figure 3 Inset shows the values of the initial velocity *vs.* oxygen concentration at very high monophenol concentrations, and from this hyperbola the $K_{m,M}^{O_2(S)}$ can be obtained. When the initial concentration of oxygen is varied and the monophenol concentration is maintained constant, no sigmoid shape is obtained for velocity *vs.* oxygen concentration (Fig. 4). The data for Figs. 3 and 4 agreed with Eqs. (8) and (9) which are obtained taking into account the rapid equilibrium. These results agreed with other isotopic effect studies demonstrated that the limiting step of the monophenolase activity corresponded to the transference of the hydroxyl proton of the monophenol (position 4) to the peroxide of *oxy*-tyrosinase, which correspond to the step controlled by k_5 (Scheme 2) [26,27].

As can be seen in Fig. 1 Inset and Fig. 3 Inset, representing the initial velocity *vs.* initial oxygen concentration provides the Michaelis constant for oxygen in the slow pathway. In the case of monophenols, we obtain $K_{m,M}^{O_2(S)}$, a very complex expression (A47): note the increasing values of the apparent Michaelis constant for oxygen in

the slow pathway compared with that obtained in the kinetically preferred pathway (Table 1).

As regards the stereochemistry, according to the results depicted in Table 1, the values for K_m^S are much higher in the D isomers compared with L, both in *o*-diphenols and monophenols. However, $K_m^{O_2(P)}$ does not vary since k_{cat} is the same, the values of δ_3 and δ_4 being the same for both isomers. The data in Table 1 shows that the values of $K_m^{O_2(S)}$ are practically the same for both isomers, although much higher than those of $K_m^{O_2(P)}$. This difference is due to the oxygen binding constant: in the kinetically preferred pathway oxygen binds to *deoxy*-tyrosinase and in the slow pathway it binds to the intermediate *deoxy*-tyrosinase/*o*-diphenol or *deoxy*-tyrosinase/monophenol.

The experimental results show that tyrosinase expresses kinetic cooperativity when it acts on *o*-diphenols, which can be explained if only one active centre exists. Furthermore, these results indicate that, in the monophenolase activity, the limiting step in the turnover is the hydroxylation of monophenols to *o*-diphenols.

Acknowledgments This paper was partially supported by grants from the Ministerio de Educación y Ciencia (Madrid, Spain) Project BIO2009-12956, from the Fundación Séneca (CARM, Murcia, Spain) Projects 08856/PI/08 and 08595/PI/08, from the Consejería de Educación (CARM, Murcia, Spain) BIO-BMC 06/01-0004 and from FISCAM PI-2007/53 from the Consejería de Salud y Bienestar Social de la Junta de Comunidades de Castilla La Mancha. J.L.M.M. has a fellowship from the Ministerio de Educación y Ciencia (Madrid, Spain) Reference AP2005-4721. F.G.M has a fellowship from Fundación Caja Murcia (Murcia, Spain).

Appendix: Analytical expressions for the equations described in the main text

The expressions of the parameters $\alpha_i (i = 1, 2, 3, 4)$ involved in Eq. (5) are:

$$\alpha_1 = \frac{2k_3k_7}{k_3 + k_7} \tag{A1}$$

$$\alpha_2 = \frac{k_3K_9K_{10}}{k_3 + k_7} \tag{A2}$$

$$\alpha_3 = \frac{k_{-2}k_7 + k_3k_7 + k_2k_3K_6}{k_2(k_3 + k_7)} \tag{A3}$$

$$\alpha_4 = \frac{k_3K_{10}}{k_3 + k_7} \tag{A4}$$

The expressions of the parameters $\beta_i (i = 1, 2, 3, \ldots, 11)$ involved in Eq. (6) are:

$$\beta_1 = k_2k_3k_8k_6k_7k_{-9} + k_2k_3k_9k_{-8}k_7k_{10} + k_2k_3k_8k_6k_7k_{-9} + k_2k_3k_9k_{-8}k_7k_{10} \tag{A5}$$

$$\beta_2 = k_2k_3k_8k_6k_7k_{10} + k_2k_3k_8k_6k_7k_{10} \tag{A6}$$

$$\beta_3 = k_2k_3k_9k_6k_7k_{10} + k_2k_3k_9k_6k_7k_{10} \tag{A7}$$

$$\beta_4 = k_2k_3k_{-8}k_7k_{-9} + k_2k_3k_{-8}k_{-6}k_{-9} + k_2k_3k_{-8}k_{-10}k_{-9} \tag{A8}$$

$$\begin{aligned}\beta_5 = {} & k_{-2}k_8k_6k_7k_{-9} + k_{-2}k_9k_{-8}k_7k_{10} + k_3k_8k_6k_7k_{-9} + k_3k_9k_{-8}k_7k_{10} \\ & + k_2k_3k_{-8}k_7k_{10} + k_2k_3k_{-8}k_{-6}k_{10} + k_2k_3k_8k_7k_{-9} + k_2k_3k_8k_{-6}k_{-9} \\ & + k_2k_3k_8k_{-10}k_{-9}\end{aligned} \tag{A9}$$

$$\beta_6 = k_2k_3k_6k_7k_{-9} + k_2k_3k_6k_{-10}k_{-9} + k_2k_3k_9k_{-8}k_7 + k_2k_3k_9k_{-8}k_{-6} + k_2k_3k_9k_{-8}k_{-10} \quad \text{(A10)}$$

$$\beta_7 = k_{-2}k_8k_6k_7k_{10} + k_3k_8k_6k_7k_{10} + k_2k_3k_8k_7k_{10} + k_2k_3k_8k_{-6}k_{10} \quad \text{(A11)}$$

$$\beta_8 = k_{-2}k_9k_6k_7k_{10} + k_3k_9k_6k_7k_{10} + k_2k_8k_6k_7k_{-9} + k_2k_9k_{-8}k_7k_{10} + k_2k_3k_6k_7k_{10} + k_2k_3k_9k_{-6}k_{10} + k_2k_3k_8k_6k_{-9} + k_2k_3k_9k_{-8}k_{10} + k_2k_3k_8k_6k_{-10} \quad \text{(A12)}$$

$$\beta_9 = k_2k_3k_9k_6k_7 + k_2k_3k_9k_6k_{-10} \quad \text{(A13)}$$

$$\beta_{10} = k_2k_8k_6k_7k_{10} + k_2k_3k_8k_6k_{10} \quad \text{(A14)}$$

$$\beta_{11} = k_2k_9k_6k_7k_{10} + k_2k_3k_9k_6k_{10} \quad \text{(A15)}$$

The expressions of the parameters $\gamma_i (i = 1, 2, 3, \ldots, 20, 21)$ involved in Eq. (7) are:

$$\gamma_1 = k_{-1}k_2k_3k_8k_4k_5k_7k_{-11} + k_{-1}k_2k_3k_8k_4k_5k_{-6}k_{-11} + k_{-1}k_2k_3k_{11}k_{-8}k_5k_7k_{12} + k_{-1}k_2k_3k_{11}k_{-8}k_5k_{-6}k_{12} \quad \text{(A16)}$$

$$\gamma_2 = k_{-1}k_2k_3k_8k_6k_5k_7k_{-11} + k_{-1}k_2k_3k_8k_6k_{-4}k_7k_{-11} + k_{-1}k_2k_3k_8k_6k_{-12}k_7k_{-11} + k_{-1}k_2k_3k_8k_6k_5k_7k_{-11} + k_{-1}k_2k_3k_8k_6k_{-4}k_7k_{-11} + k_{-1}k_2k_3k_8k_6k_{-12}k_7k_{-11} \quad \text{(A17)}$$

$$\gamma_3 = k_{-1}k_2k_3k_{11}k_4k_5k_7k_{12} + k_{-1}k_2k_3k_{11}k_4k_5k_{-6}k_{12} \quad \text{(A18)}$$

$$\gamma_4 = k_{-1}k_2k_3k_8k_4k_5k_7k_{12} + k_{-1}k_2k_3k_8k_4k_5k_{-6}k_{12} \quad \text{(A19)}$$

$$\gamma_5 = k_{-1}k_2k_3k_{11}k_6k_5k_7k_{12} + k_{-1}k_2k_3k_{11}k_6k_{-4}k_7k_{12} + k_{-1}k_2k_3k_{11}k_6k_{-4}k_7k_{12} \quad \text{(A20)}$$

$$\gamma_6 = k_{-1}k_2k_3k_8k_6k_5k_7k_{12} + k_{-1}k_2k_3k_8k_6k_{-4}k_7k_{12} + k_{-1}k_2k_3k_8k_6k_5k_7k_{12} + k_{-1}k_2k_3k_8k_6k_{-4}k_7k_{12} \quad \text{(A21)}$$

$$\gamma_7 = k_{-1}k_2k_3k_{-8}k_5k_7k_{-11} + k_{-1}k_2k_3k_{-8}k_5k_{-6}k_{-11} + k_{-1}k_2k_3k_{-8}k_{-4}k_7k_{-11} + k_{-1}k_2k_3k_{-8}k_{-4}k_{-6}k_{-11} + k_{-1}k_2k_3k_{-8}k_{-12}k_7k_{-11} + k_{-1}k_2k_3k_{-8}k_{-12}k_{-6}k_{-11} \quad \text{(A22)}$$

$$\gamma_8 = k_{-1}k_2k_3k_4k_5k_7k_{-11} + k_{-1}k_2k_3k_4k_5k_{-6}k_{-11} + k_{-1}k_2k_3k_4k_{-12}k_7k_{-11} + k_{-1}k_2k_3k_4k_{-12}k_{-6}k_{-11} + k_{-1}k_2k_3k_{11}k_{-8}k_5k_7 + k_{-1}k_2k_3k_{11}k_{-8}k_5k_{-6} + k_{-1}k_2k_3k_{11}k_{-8}k_{-4}k_7 + k_{-1}k_2k_3k_{11}k_{-8}k_{-4}k_{-6} + k_{-1}k_2k_3k_{11}k_{-8}k_{-12}k_7 + k_{-1}k_2k_3k_{11}k_{-8}k_{-12}k_{-6} \quad \text{(A23)}$$

$$\gamma_9 = k_{-1}k_{-2}k_8k_4k_5k_7k_{-11} + k_{-1}k_{-2}k_8k_4k_5k_{-6}k_{-11} + k_{-1}k_{-2}k_{11}k_{-8}k_5k_7k_{12} + k_{-1}k_{-2}k_{11}k_{-8}k_5k_{-6}k_{12} + k_{-1}k_{-2}k_3k_{-8}k_5k_7k_{12} + k_{-1}k_2k_3k_{-8}k_5k_{-6}k_{12} + k_{-1}k_2k_3k_{-8}k_{-4}k_7k_{12} + k_{-1}k_2k_3k_{-8}k_{-4}k_{-6}k_{12} + k_{-1}k_2k_3k_8k_5k_7k_{-11} + k_{-1}k_2k_3k_8k_5k_{-6}k_{-11} + k_{-1}k_2k_3k_8k_{-4}k_7k_{-11} + k_{-1}k_2k_3k_8k_{-4}k_{-6}k_{-11} + k_{-1}k_2k_3k_8k_{-12}k_7k_{-11} + k_{-1}k_2k_3k_8k_{-12}k_{-6}k_{-11} \quad \text{(A24)}$$

$$\gamma_{10} = k_{-1}k_2k_3k_6k_5k_7k_{-11} + k_{-1}k_2k_3k_6k_{-4}k_7k_{-11} + k_{-1}k_2k_3k_6k_{-12}k_7k_{-11} \quad \text{(A25)}$$

$$\gamma_{11} = k_{-1}k_{-2}k_8k_6k_5k_7k_{-11} + k_{-1}k_{-2}k_8k_6k_{-4}k_7k_{-11} + k_{-1}k_{-2}k_8k_6k_{-12}k_7k_{-11} + k_{-1}k_3k_8k_6k_5k_7k_{-11} + k_{-1}k_3k_8k_6k_{-4}k_7k_{-11} + k_{-1}k_3k_8k_6k_{-12}k_7k_{-11} \tag{A26}$$

$$\gamma_{12} = k_{-1}k_2k_3k_{11}k_4k_5k_7 + k_{-1}k_2k_3k_{11}k_4k_5k_{-6} + k_{-1}k_2k_3k_{11}k_4k_{-12}k_7 + k_{-1}k_2k_3k_{11}k_4k_{-12}k_{-6} \tag{A27}$$

$$\gamma_{13} = k_1k_{-2}k_8k_4k_5k_7k_{-11} + k_1k_{-2}k_8k_4k_5k_{-6}k_{-11} + k_1k_{-2}k_{11}k_{-8}k_5k_7k_{12} + k_1k_{-2}k_{11}k_{-8}k_5k_{-6}k_{12} + k_{-1}k_{-2}k_{11}k_4k_5k_7k_{12} + k_{-1}k_{-2}k_{11}k_4k_5k_{-6}k_{12} + k_{-1}k_2k_8k_4k_5k_7k_{-11} + k_{-1}k_2k_8k_4k_5k_{-6}k_{-11} + k_{-1}k_2k_{11}k_{-8}k_5k_7k_{12} + k_{-1}k_2k_{11}k_{-8}k_5k_{-6}k_{12} + k_{-1}k_2k_3k_4k_5k_7k_{12} + k_{-1}k_2k_3k_4k_5k_{-6}k_{12} + k_{-1}k_2k_3k_{11}k_{-4}k_7k_{12} + k_{-1}k_2k_3k_{11}k_{-4}k_{-6}k_{12} + k_{-1}k_2k_3k_8k_4k_7k_{-11} + k_{-1}k_2k_3k_8k_4k_{-6}k_{-11} + k_{-1}k_2k_3k_{11}k_{-8}k_7k_{12} + k_{-1}k_2k_3k_{11}k_{-8}k_{-6}k_{12} + k_{-1}k_2k_3k_8k_4k_{-12}k_7 + k_{-1}k_2k_3k_8k_4k_{-12}k_{-6} \tag{A28}$$

$$\gamma_{14} = k_{-1}k_{-2}k_8k_4k_5k_7k_{12} + k_{-1}k_{-2}k_8k_4k_5k_{-6}k_{12} + k_{-1}k_2k_3k_8k_5k_7k_{12} + k_{-1}k_2k_3k_8k_5k_{-6}k_{12} + k_{-1}k_2k_3k_8k_{-4}k_7k_{12} + k_{-1}k_2k_3k_8k_{-4}k_{-6}k_{12} \tag{A29}$$

$$\gamma_{15} = k_{-1}k_2k_3k_{11}k_6k_5k_7 + k_{-1}k_2k_3k_{11}k_6k_{-4}k_7 + k_{-1}k_2k_3k_{11}k_6k_{-12}k_7 \tag{A30}$$

$$\gamma_{16} = k_1k_{-2}k_8k_6k_5k_7k_{-11} + k_1k_{-2}k_8k_6k_{-4}k_7k_{-11} + k_1k_{-2}k_8k_6k_{-12}k_7k_{-11} + k_1k_3k_8k_6k_5k_7k_{-11} + k_1k_3k_8k_6k_{-4}k_7k_{-11} + k_1k_3k_8k_6k_{-12}k_7k_{-11} + k_{-1}k_{-2}k_{11}k_6k_5k_7k_{12} + k_{-1}k_{-2}k_{11}k_6k_{-4}k_7k_{12} + k_{-1}k_3k_{11}k_6k_{-4}k_7k_{-12} + k_{-1}k_2k_8k_6k_5k_7k_{-11} + k_{-1}k_2k_8k_6k_{-4}k_7k_{-11} + k_{-1}k_2k_8k_6k_{-12}k_7k_{-11} + k_{-1}k_2k_3k_6k_5k_7k_{12} + k_{-1}k_2k_3k_6k_{-4}k_7k_{12} + k_{-1}k_2k_3k_8k_6k_5k_{-11} + k_{-1}k_2k_3k_8k_6k_{-4}k_{-11} + k_{-1}k_2k_3k_8k_6k_{-12}k_{-11} \tag{A31}$$

$$\gamma_{17} = k_{-1}k_{-2}k_8k_6k_5k_7k_{12} + k_{-1}k_{-2}k_8k_6k_{-4}k_7k_{12} + k_{-1}k_3k_8k_6k_5k_7k_{12} + k_{-1}k_3k_8k_6k_{-4}k_7k_{12} \tag{A32}$$

$$\gamma_{18} = k_1k_{-2}k_{11}k_4k_5k_7k_{12} + k_1k_{-2}k_{11}k_4k_5k_{-6}k_{12} + k_{-1}k_2k_{11}k_4k_5k_7k_{12} + k_{-1}k_2k_{11}k_4k_5k_{-6}k_{12} + k_{-1}k_2k_3k_{11}k_4k_7k_{12} + k_{-1}k_2k_3k_{11}k_4k_{-6}k_{12} \tag{A33}$$

$$\gamma_{19} = k_1k_{-2}k_8k_4k_5k_7k_{12} + k_1k_{-2}k_8k_4k_5k_{-6}k_{12} + k_{-1}k_2k_8k_4k_5k_7k_{12} + k_{-1}k_2k_8k_4k_5k_{-6}k_{12} + k_{-1}k_2k_3k_8k_4k_7k_{12} + k_{-1}k_2k_3k_8k_4k_{-6}k_{12} \tag{A34}$$

$$\gamma_{20} = k_1k_{-2}k_{11}k_6k_5k_7k_{12} + k_1k_{-2}k_{11}k_6k_{-4}k_7k_{12} + k_1k_3k_{11}k_6k_{-4}k_7k_{12} + k_{-1}k_2k_{11}k_6k_5k_7k_{12} + k_{-1}k_2k_{11}k_6k_{-4}k_7k_{12} + k_{-1}k_2k_3k_{11}k_6k_7k_{12} + k_{-1}k_2k_3k_{11}k_6k_{-4}k_{12} \tag{A35}$$

$$\gamma_{21} = k_1k_{-2}k_8k_6k_5k_7k_{12} + k_1k_{-2}k_8k_6k_{-4}k_7k_{12} + k_1k_3k_8k_6k_5k_7k_{12} + k_1k_3k_8k_6k_{-4}k_7k_{12} + k_{-1}k_2k_8k_6k_5k_7k_{12} + k_{-1}k_2k_8k_6k_{-4}k_7k_{12} + k_{-1}k_2k_3k_8k_6k_5k_{12} + k_{-1}k_2k_3k_8k_6k_{-4}k_{12} \tag{A36}$$

The expressions of the parameters $\varphi_i (i = 1, 2, 3 \ldots 9)$ involved in Eq. (8) are:

$$\varphi_1 = K_1 k_2 k_3 k_5 k_7 + K_1 k_2 k_3 k_5 k_{-6} \tag{A37}$$
$$\varphi_2 = K_1 k_2 k_3 k_6 K_4 k_7 + K_1 k_2 k_3 k_6 K_4 k_7 \tag{A38}$$
$$\varphi_3 = K_1 k_2 k_3 K_8 K_4 k_7 + K_1 k_2 k_3 K_8 K_4 k_{-6} \tag{A39}$$
$$\varphi_4 = K_1 k_{-2} k_5 k_7 + K_1 k_{-2} k_5 k_{-6} \tag{A40}$$
$$\varphi_5 = K_1 k_2 k_3 K_{12} k_7 + K_1 k_2 k_3 K_{12} k_{-6} \tag{A41}$$
$$\varphi_6 = K_1 k_{-2} k_6 K_4 k_7 + K_1 k_3 k_6 K_4 k_7 + K_1 k_2 k_3 K_4 k_7 + K_1 k_2 k_3 K_4 k_{-6} \tag{A42}$$
$$\varphi_7 = k_{-2} k_5 k_7 + k_{-2} k_5 k_{-6} \tag{A43}$$
$$\varphi_8 = k_{-2} k_6 K_4 k_7 + k_3 k_6 K_4 k_7 + K_1 k_2 k_5 k_7 + K_1 k_2 k_5 k_{-6} + K_1 k_2 k_3 k_7 + K_1 k_2 k_3 k_{-6} \tag{A44}$$
$$\varphi_9 = K_1 k_2 k_6 K_4 k_7 + K_1 k_2 k_3 k_6 K_4 \tag{A45}$$

The analytical expression for R is:

$$R = \frac{k_{\text{cat}}^{M} K_m^{D(P)}}{2 k_{\text{cat}}^{D} K_m^{M(P)}} = \frac{k_4}{2 k_6} \tag{A46}$$

Taking into account the Eqs. (A46) and Eqs. (A41), (A43), (A44) and (A45), $K_m^{O_2(S)}$ in the monophenolase activity, is:

$$K_m^{O_2(S)} = \frac{\varphi_5 R}{\varphi_7 + \varphi_8 R + \varphi_9 R^2} \tag{A47}$$

References

1. A. Cornish-Bowden, in *Fundamentals of enzyme kinetics*, ed. by A. Cornish-Bowden (Butterworths, London, 1979), pp. 172–175
2. R.B. Silverman, in *Contemporary enzyme kinetics and mechanism*, ed. by D.L. Purich (San Diego, 2009), pp. 246–248
3. W. Ferdinand, in *The enzyme molecule*, ed. by W. Ferdinand (John Wiley and Sons, London, 1976), pp. 139–185
4. D. Atkinson, G.M. Walton, J. Biol. Chem. **240**, 757 (1965)
5. J.A. Hathaway, D.E. Atkinson, J. Biol. Chem. **238**, 2875 (1963)
6. R.G. Wolfe, J.B. Neilands, J. Biol. Chem. **221**, 61 (1956)
7. E.I. Solomon, U.M. Sundaram, T.E. Machonkin, Chem. Rev. **96**, 2563 (1996)
8. R.L. Jolley, L.H. Evans, N. Makino, H.S. Mason, J. Biol. Chem. **249**, 335 (1974)
9. Y. Matoba, T. Kumagai, A. Yamamoto, H. Yoshitsu, M. Sugiyama, J. Biol. Chem. **281**, 8981 (2006)
10. H. Decker, T. Schweikardt, F. Tuczek, Angew. Chem. Int. Ed. **45**, 4546 (2006)
11. R.J. Deeth, C. Diedrich, J. Biol. Inorg. Chem. **15**, 117 (2010)
12. A. Sanchez-Ferrer, J.N. Rodriguez-Lopez, F. Garcia-Canovas, F. Garcia-Carmona, Biochim. Biophys. Acta **1247**, 1 (1995)
13. F. Garcia-Molina, J.L. Munoz, R. Varon, J.N. Rodriguez-Lopez, F. Garcia-Canovas, J. Tudela, J. Agric. Food Chem. **55**, 9739 (2007)
14. L.G. Fenoll, J.N. Rodriguez-Lopez, F. Garcia-Sevilla, P.A. Garcia-Ruiz, R. Varon, F. Garcia-Canovas, J. Tudela, Biochim. Biophys. Acta **1548**, 1 (2001)

15. J.N. Rodriguez-Lopez, J. Tudela, R. Varon, F. Garcia-Carmona, F. Garcia-Canovas, J. Biol. Chem. **267**, 3801 (1992)
16. J.L. Munoz-Munoz, F. Garcia-Molina, R. Varon, J. Tudela, F. Garcia-Canovas, J.N. Rodriguez-Lopez, Biochim. Biophys. Acta **1794**, 1017 (2009)
17. J.N. Rodriguez-Lopez, L.G. Fenoll, P.A. Garcia-Ruiz, R. Varon, J. Tudela, R.N. Thorneley, F. Garcia-Canovas, Biochemistry **39**, 10497 (2000)
18. M.M. Bradford, Anal. Biochem. **72**, 248 (1976)
19. F. Garcia-Carmona, F. Garcia-Canovas, J.L. Iborra, J.A. Lozano, Biochim. Biophys. Acta **717**, 124 (1982)
20. F. Garcia-Canovas, F. Garcia-Carmona, J. Vera-Sanchez, J.L. Iborra, J.A. Lozano, J. Biol. Chem. **257**, 8738 (1982)
21. J.L. Munoz, F. Garcia-Molina, R. Varon, J.N. Rodriguez-Lopez, F. Garcia-Canovas, J. Tudela, Anal. Biochem. **351**, 128 (2006)
22. J.N. Rodriguez-Lopez, J.R. Ros-Martinez, R. Varon, F. Garcia-Canovas, Anal. Biochem. **202**, 356 (1992)
23. Jandel Scientific, Sigma Plot 9.0 for Windows^{TM}; Jandel Scientific: Core Madera (2006)
24. E. Van Schaftingen, M.-F. Jet, L. Hue, H.-G. Hers, Proc. Natl. Acad. Sci. USA **78**, 3483 (1981)
25. J.R. Ros, J.N. Rodriguez-Lopez, F. Garcia-Canovas, Biochim. Biophys. Acta **1204**, 33 (1994)
26. L.G. Fenoll, M.J. Peñalver, J.N. Rodriguez-Lopez, P.A. Garcia-Ruiz, F. Garcia-Canovas, J. Tudela, Biochem. J. **380**, 643 (2004)
27. M.J. Peñalver, J.N. Rodriguez-Lopez, P.A. Garcia-Ruiz, F. Garcia-Canovas, J. Tudela, Biochim. Biophys. Acta **1650**, 128 (2003)